Rearrangements in Negatively Charged Ammonium Nitrate Clusters

ARTICLE *in* THE JOURNAL OF PHYSICAL CHEMISTRY · AUGUST 1994

Impact Factor: 2.78 · DOI: 10.1021/j100085a001

2 AUTHORS, INCLUDING:

Brett I. Dunlap
United States Naval Research Laboratory
185 PUBLICATIONS **7,623** CITATIONS

The Journal of Physical Chemistry

 VOLUME 98, NUMBER 34, AUGUST 25, 1994

LETTERS

Rearrangements in Negatively Charged Ammonium Nitrate Clusters

Robert J. Doyle, Jr.,* and Brett I. Dunlap

Chemistry Division, Code 6100, Naval Research Laboratory, Washington, DC 20375-5000

Received: April 6, 1994; In Final Form: June 10, 1994®

The sputtering of condensed-phase ammonium nitrate yields an extensive distribution of cluster ions with the general formula $[NH_4NO_3)_nNO_3]^-$, where $n = 3$ to >40. Only a very low relative abundance of the $n = 1$ and the $n = 2$ species are detected by mass spectrometry. Collision-induced dissociation experiments suggest that $[NH_4NO_3)NO_3]^-$ rearranges to lose NH_3 and form $[H(NO_3)_2]^-$, which is detected at high relative abundance. Gradient-corrected density functional calculations show that there is strong hydrogen bonding in NH_4NO_3 and essentially no hydrogen bonding in $[NH_4NO_3)NO_3]^-$. Thus, with a relatively small amount of internal energy the latter can rearrange to lose a neutral ammonia molecule.

Introduction

It has been demonstrated that high-energy sputtering of condensed-phase ammonium nitrate (AN) produces a mass spectrum of positive AN cluster ions of the general formula $[(NH_4NO_3)_nNH_4]^+$, where $n = 1$ to >43 inclusive.[1] Within the AN cluster ion distribution, cluster ions with all values of n were detected. Local variations in ion abundance over a small range of n were within a dynamic range of about an order of magnitude. Large local variations are caused by significant differences in the relative stabilities of those ions. Often, this is a consequence of an ion losing neutral units (NH_4NO_3, in this case) to form a more stable cluster ion with a closed solvent shell.[2] Of particular interest was the observation of a competitive dissociation pathway that involved the loss of HNO_3 through rearrangement of small AN cluster ions ($n = 1$–6). As will be shown, small negatively charged AN cluster ions ($[(NH_4NO_3)_nNO_3]^-$) also undergo dissociative rearrangements that are competitive with dissociations that occur by loss of NH_4NO_3. In the case of negative AN cluster ions, however, the rearrangement results in the loss of NH_3. Both the mass spectrum of sputtered AN^- cluster ions and the collision-induced dissociation spectra of a series ($n = 3$–14) of gas-phase AN^- cluster ions show that this reaction becomes more favorable as cluster size decreases. As a result, the two smallest cluster ions are detected only in trace amounts. The evidence shows that a high percentage of the ion populations of the $n = 1$ and $n = 2$ clusters have rearranged and lost NH_3 prior to detection.

Experimental Section

Negatively charged AN cluster ions, of the general formula $[(NH_4NO_3)_nNO_3]^-$, where $n = 3$ to >40 inclusive, were generated by high-energy sputtering. The negative ion mass spectrum of sputtered AN is shown in Figure 1. As noted above, the first two cluster ions of the series ($n = 1$ and $n = 2$) are present in trace amounts only. The absence of $n = 1$ is all the more surprising because $n = 1$ would be expected to be the core ion upon which all larger clusters are built . In addition to the absence of the $n = 1$ and 2 ions, three further points are to be made: (1) from $n = 3$ to $n = 40$, all cluster ions in the series $[(NH_4NO_3)_nNO_3]^-$ are observed; (2) intermediate cluster ions (Figure 1: a, b, and c) are formed by losses of NH_3 from $[(NH_4NO_3)_nNO_3]^-$ ions (in significant abundances only from ions with $n < 8$), and (3) the protonated nitrate clusters, $[H(NO_3)_2]^-$ and $[H_2(NO_3)_3]^-$, are abundant in the low-mass region of the spectrum. Items 2 and 3 suggest that $[H(NO_3)_2]^-$ and $[H_2(NO_3)_3]^-$ could be formed by the loss of NH_3 from $[(NH_4NO_3)NO_3]^-$ and from the loss of

* Abstract published in *Advance ACS Abstracts*, August 1, 1994.

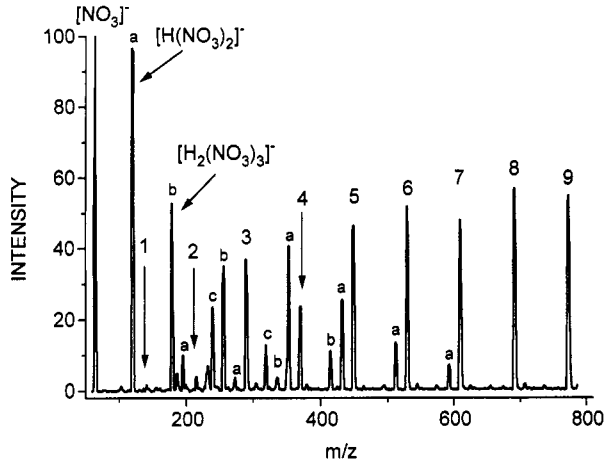

Figure 1. Partial negative-ion mass spectrum of sputtered ammonium nitrate. Index numbers for $[(NH_4NO_3)_nNO_3]^-$ ions are indicated. Losses of one, two, and three NH_3 molecules are indicated by a, b, and c, respectively. The losses occur from the adjacent $[(NH_4NO_3)_nNO_3]^-$ ion with the highest value of n.

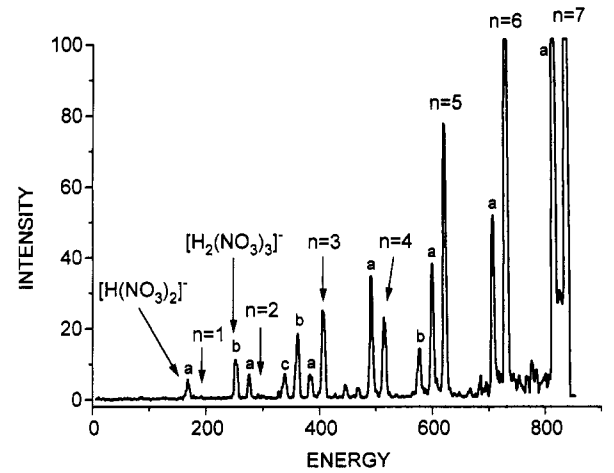

Figure 2. CID spectrum of $[(NH_4NO_3)_7NO_3]^-$. Index numbers for $[(NH_4NO_3)_nNO_3]^-$ product ions are indicated. Losses of NH_3 are designated a, b, and c, as in Figure 1.

$2NH_3$ from $[(NH_4NO_3)_2NO_3]^-$, respectively. In other words, a fast dissociation reaction at the sample surface or in the gas phase results in a low yield of the $n = 1$ and the $n = 2$ species. Cluster ions predominantly dissociate by consecutive losses of the neutral unit with which the cluster is built,[3] in this case NH_4NO_3, and yield the smaller cluster ions, including the $n = 1$ core ion. The dissociation of mass-selected $[(NH_4NO_3)_nNO_3]^-$ gas-phase cluster ions can be observed by collision-induced dissociation[4] (CID). This technique permits another avenue of approach to resolving the problem of the missing cluster ions. In contrast to the mass spectrum, which identifies clusters desorbed from a surface, CID produces smaller cluster ions from larger preformed gas-phase cluster ions.

The CID spectrum of $[(NH_4NO_3)_7NO_3]^-$ is shown in Figure 2. With the collision-gas pressure maintained in the multiple-collision region, extensive dissociation of the reactant ion occurs.[5] The spectrum shows multiple losses of the principal neutral unit, NH_4NO_3, from the $n = 7$ parent ion, yielding the fragment ions $n = 6$, 5, 4, and 3. The $n = 1$ and 2 fragment ions are detected only in trace amounts, similar to the negative-ion mass spectrum of AN (Figure 1), where they were observed in a somewhat lower relative abundance. Intermediate fragment ions (a, b, and c), formed by losses of NH_3 from $[(NH_4NO_3)_nNO_3]^-$ ions, are observed in relative abundances that are very similar to those observed in the mass spectrum (Figure 1). The salient point is that a very low abundance of $n = 1$ and $n = 2$ ions is observed, and this is seen in the CID spectra of all $[(NH_4NO_3)_nNO_3]^-$ ions from $n = 3$–14.[6] In each case the ion abundance distribution is similar to that in Figure 2: an exponential decrease in the abundance of $[(NH_4NO_3)_nNO_3]^-$ fragment ions that plateaus at $n = 4$ and $n = 3$. The sharp cutoff at $n = 2$ is seen for all parent cluster ions. The fact that *some* $n = 1$ and $n = 2$ ions are detected suggests that these ions may indeed form but then rapidly dissociate by the loss (or losses) of NH_3. The sharp cutoff at $n = 2$ seems to indicate that the dissociation of the $n = 1$ and $n = 2$ species is controlled to a greater degree by mechanistic effects rather than internal energy effects. The latter would be expected to show a more continuous decrease in fragment ion abundance due to the evaporation of the monomer units (NH_4NO_3) from the mass-selected cluster ions. Three reactions are proposed for the dissociation of the $n = 1$ and $n = 2$ species by losses of NH_3. For the $n = 1$ ion, the reaction is

$$[(NH_4NO_3)NO_3]^- \rightarrow [H(NO_3)_2]^- + NH_3 \quad (1)$$

the product of which is observed in both Figures 1 and 2. For the $n = 2$ ion, the following reactions would occur:

$$[(NH_4NO_3)_2NO_3]^- \rightarrow [H(NH_4NO_3)(NO_3)_2]^- + NH_3 \quad (2)$$

$$[(NH_4NO_3)_2NO_3]^- \rightarrow [H_2(NO_3)_3]^- + 2NH_3 \quad (3)$$

The products of reactions 2 and 3 are also observed in Figures 1 and 2.

It is convenient to examine the simplest system, reaction 1, in detail. As a first approximation for the ensuing calculations, the reactant ion, $[(NH_4NO_3)NO_3]^-$, might be assumed to have a structure consisting of a central ammonium ion hydrogen-bonded to two nitrate anions. If the nitrate anions are bonded to separate hydrogen atoms of the ammonium ion, then the structure must rearrange in order to lose NH_3. On the other hand, if both nitrate anions are bonded to the same hydrogen atom of the ammonium ion, NH_3 would be loosely bonded and therefore easily lost. In a similar situation involving the mixed cluster ions $[(C_5H_5N)_n$-$NH_4]^+$, it was reported that the $n = 2$ species (analogous to $n = 1$ for $[(NH_4NO_3)NO_3]^-$) had both pyridine molecules bonded to the same hydrogen atom of the ammonium ion.[7] It loses NH_3 directly. The $n = 3$ species, however, has three pyridine molecules hydrogen-bonded to three different hydrogen atoms of the ammonium ion and undergoes intracluster molecular rearrangement to lose NH_3. Because no thermodynamic quantities have been reported for any of the ions in reactions 1–3, we will rely upon a purely theoretical approach to understanding these hydrogen-bonded systems. Ions and molecules as large as $[(NH_4NO_3)NO_3]^-$ can be treated from first principles.

Calculations

Density functional theory[8] is an appropriate method to use to study these hydrogen-bonded systems. Gradient-corrected functionals are important in this work which relies on total energies.[9] The deMon computer code[10,11] uses Gaussian bases for the orbitals and the electronic potential,[12] and a variational principle makes four-center integrals unnecessary.[13] The default double-zeta plus polarization on heavy atoms basis set was used with the Becke–Perdew[14,15] exchange and correlation potential. The geometries were optimized using this basis and potential combination, and the resultant total energies for selected molecules and ions are listed in Table 1.

The optimized structure of the monomer unit NH_4NO_3 is compared to the optimized structure of the $n = 1$ negative ion $[(NH_4NO_3)NO_3]^-$ in Figure 3. The structure of NH_4NO_3 is quite similar to that found in *ab initio* calculations.[16] The hydrogen bond in the monomer is one of the strongest known. The four hydrogen atoms are not bound the same way; one hydrogen atom is pulled away from the nitrogen atom of the

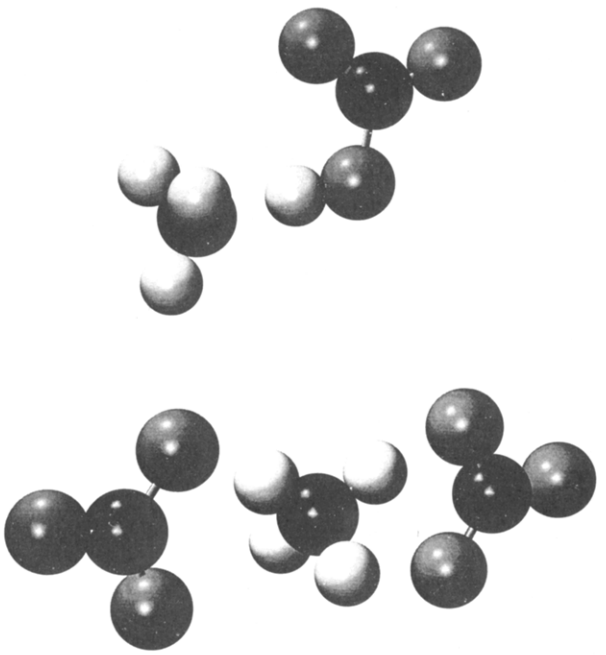

Figure 3. Optimized gradient-corrected density functional structure of NH_4NO_3 above and $[(NH_4NO_3)NO_3]^-$ below. Nitrogen, oxygen, and hydrogen are indicated by successively lighter shades of gray. Note that one hydrogen atom is closer to an oxygen atom than it is to the nitrogen atom in NH_4NO_3 but that all the hydrogen atoms are bonded to the nitrogen atom in $[(NH_4NO_3)NO_3]^-$.

TABLE 1: Becke–Perdew Total Molecular Energies in hartree Atomic Units

species	energy	species	energy
NH_3	−56.5703	NH_4NO_3	−337.5876
NH_4^+	−56.9104	$[H(NO_3)_2]^-$ (C_{2h})	−561.5085
NO_3^-	−280.4672	$[(NH_4NO_3)NO_3]^-$	−618.1067

ammonium ion to the closest oxygen atom. In contrast, there are no strong hydrogen bonds in $[(NH_4NO_3)NO_3]^-$, where the bonding is almost purely ionic. The nitrogen atoms are essentially collinear—far from the roughly tetrahedral angle one might expect if the nitrate ions were strongly interacting with neighboring hydrogen atoms. This can be quantified using the energies of Table 1. The dissociation energy of $[(NH_4NO_3)NO_3]^-$, the energy needed to separate it into three ions, is 0.258 hartree atomic units. The energy of a row of three electronic charges that alternate in sign and have nearest-neighbor distance R is $3/(2R)$ in atomic units. Equating the two energies and solving for R yields 5.8 a_0. The optimized average nearest-neighbor N–N distances in $[(NH_4NO_3)NO_3]^-$ and NH_4NO_3 are 6.1 and 6.3 a_0, respectively. The binding energy of NH_4NO_3 is 0.210 hartree, considerably larger than $1/R$, which is 0.159 hartree. The extra 0.051 hartree (32 kcal/mol) is roughly the hydrogen-bond energy. The calculated dipole moment is large, 6.06 D, but not the 16 D that a completely ionic model would predict. Because the hydrogen bond is eliminated, associating NH_4NO_3 and NO_3^- gains only 0.052 hartree (33 kcal/mol). Furthermore, there is another association/dissociation pathway, that of reaction 1. For $H(NO_3)_2^-$ two isomers[17] were optimized. The C_{2h} isomer, which has its C_2 axis perpendicular to the plane of the molecule, is shown in Figure 4. This isomer is almost isoenergetic with the C_2 isomer, which has its C_2 axis in the plane of the molecule. Dissociation of NH_3 from $[(NH_4NO_3)NO_3]^-$ to leave the C_{2h} isomer is calculated to require only 0.028 hartree (18 kcal/mol). This is roughly half the energy required to dissociate NO_3^- from $[(NH_4NO_3)NO_3]^-$ and thus would be expected to be the dominant dissociation pathway.

Thus, one can imagine a process in which NH_4NO_3 and NO_3^- come together. The system gains 33 kcal/mol, and the ions vibrate and bend. Eventually, oxygen atoms from each of the two nitrate

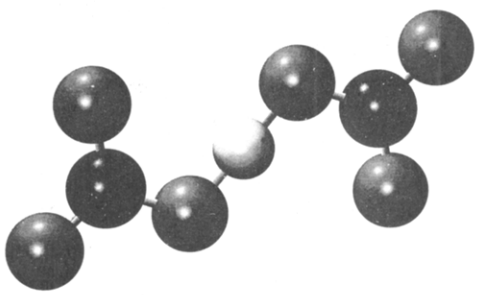

Figure 4. Optimized gradient-corrected density functional structure of the lowest energy C_{2h} isomer of $H(NO_3)_2^-$. Nitrogen, oxygen, and hydrogen are indicated by successively lighter shades of gray.

ions bond to one hydrogen atom, in one of the many possible ways that can be imagined considering the structure of $[(NH_4NO_3)NO_3]^-$ show in Figure 3. The system can then dissociate into NH_3 and $H(NO_3)_2^-$. After this dissociative rearrangement, the two molecules can separate with an excess 15 kcal/mol partitioned between internal and translational energy. As more polar monomer units surround an ammonium ion, however, more and more solvation energy is gained, and eventually the $[(NH_4NO_2)_nNO_3]^-$ ions dominate the negative-ion spectrum as one would expect.

Acknowledgment. B.I.D. thanks Dennis Salahub for inclusion in the deMon collaboration and Jan Andzelm and Andreas Koester for examples and advice on how to use the code. This work was supported by the Propulsion and Energetic Materials Program of the Mechanics Division of the Office of Naval Research, the Physics Division (Contract #N0001494WX23009), and the Naval Research Laboratory Energetic Materials Accelerated Research Initiative.

References and Notes

(1) Doyle, R. J., Jr. *J. Am. Chem. Soc.* **1993**, *115*, 5300–5301. Doyle, R. J., Jr. *J. Am. Chem. Soc.* **1994**, *116*, 3005–3011. Mass spectra were obtained using a ZAB-2F (VG Analytical Ltd.) reverse-geometry, double-focusing mass spectrometer operated with an accelerating potential of 8 kV. Ammonium nitrate samples were pressed into indium foil affixed to the tip of a fast atom bombardment probe. Xenon atoms with an average kinetic energy of 6.5 keV were generated by a saddle-field gun operated at 8 kV with an ion current of 1.5 mA. The xenon neutral current equivalent was approximately 7 μA applied to a target area of 4 mm².

(2) Keesee, R. G.; Castleman, A. W. In *Ion and Cluster Ion Spectroscopy and Structure*; Maier, J. P., Ed.; Elsevier: New York, 1989; pp 275–327.

(3) Doyle, R. J., Jr.; Campana J. E.; Eyler, J. R. *J. Phys. Chem.* **1985**, *89*, 5285–5288. Doyle, R. J., Jr.; Campana, J. E. *J. Phys. Chem.* **1985**, *89*, 4251–4256. Campana, J. E.; Doyle, R. J., Jr. *J. Chem. Soc., Chem. Commun.* **1985**, *2*, 45–46.

(4) McLafferty, F. W. *Tandem Mass Spectrometry*; Wiley: New York, 1983. Cooks, R. G. *Collision Spectroscopy*; Plenum: New York, 1978. Cooks, R. G.; Beynon, J. H.; Caprioli, R. M.; Lester, G. R. *Metastable Ions*; Elsevier: New York, 1973.

(5) CID spectra were obtained under multiple-collision conditions with the collision gas (He) maintained at a pressure sufficient to reduce the reactant ion signal by 80%. Experimental details can be found in: Doyle, R. J., Jr. *J. Am. Chem. Soc.* **1988**, *110*, 4120–4126. Doyle, R. J., Jr. *Org. Mass Spectrom.* **1993**, *28*, 83–91.

(6) Doyle, R. J., Jr. Manuscript in preparation.

(7) Wei, S.; Tzeng, W. B.; Keesee, R. G.; Castleman, A. W., Jr. *J. Am. Chem. Soc.* **1991**, *113*, 1960–1969.

(8) Parr, R. G.;Yang, W. *Density Functional Theory of Atoms and Molecules*; Oxford University Press: Oxford, 1989.

(9) Andzelm, J.; Wimmer, E. *J. Chem. Phys.* **1992**, *96*, 1280.

(10) St-Amant, A.; Salahub, D. R. *Chem. Phys. Lett.* **1990**, *169*, 387.

(11) Salahub, D. R.; Fournier, R.; Mlynarski, P.; Papai, I.; St.-Amant, A.; Ushio, J. In *Density Functional Methods in Chemistry*; Labanowski, J., Andzelm, J., Eds.; Springer: New York, 1991; p 77.

(12) Sambe, H.; Felton, H. *J. Chem. Phys.* **1975**, *62*, 1122.

(13) Dunlap, B. I.; Connolly, J. W. D.; Sabin, J. R. *J. Chem. Phys.* **1979**, *71*, 3396, 4993.

(14) Becke, A. D. *Phys. Rev. A* **1988**, *38*, 3098.

(15) Perdew, J. P. *Phys. Rev. B* **1986**, *33*, 8822.

(16) Latajka, Z.; Szczesniak, M. M.; Ratajczak, H.; Orville-Thomas, W. J. *J. Comput. Chem.* **1980**, *1*, 417.

(17) Barlic, B.; Hadz, D.; Orel, B. *Spectrochim. Acta* **1981**, *37A*, 1047.